



Estimation of Seismically Induced Longitudinal Strain in Pipelines Subjected to Incident Shear Wave

Se-Woong Yoon^a, Sang-Jin Kim^b, and Duhee Park^{✉ a}

^aMember, Dept. of Civil and Environmental Engineering, Hanyang University, Seoul 04763, Korea

^bDept. of Civil and Environmental Engineering, Hanyang University, Seoul 04763, Korea

ARTICLE HISTORY

Received 20 August 2019
Revised 25 February 2020
Accepted 19 April 2020
Published Online 3 July 2020

KEYWORDS

Pipeline
Longitudinal strain
Time-history analysis
Peak displacement
Seismic response

ABSTRACT

For buried pipelines, the longitudinal strain is the primary seismic design parameter. The strain can be calculated from a three dimensional (3D) time history analysis. However, performing a 3D analysis in practice can be prohibitive. The objective of the study is to provide guidelines for performing a simplified pseudo-static analysis that approximates the output of a 3D nonlinear analysis. A parametric study is performed to evaluate the degree of influence of numerous variables on the calculated longitudinal strain, the results of which are used to sculpture the guidelines. It is recommended to utilize the outputs from a one-dimensional site response analysis and the closed-form equations to calculate the axial and bending strains of pipelines subjected to a harmonic wave propagating at an incident angle to the longitudinal axis of the structure. To represent a transient earthquake motion as an equivalent harmonic motion, a procedure to extract the pulse that induces the maximum strain considering both the amplitude and the duration is presented. Using the proposed procedure, it is revealed that the reliability of the predicted longitudinal strain is acceptable for design purposes.

1. Introduction

Pipelines are essential lifeline facilities that provide important civil services to urban communities. Because the effect of damage in lifeline structure can propagate across the entire system, pipelines should be designed to withstand severe earthquakes. Embedded structures including pipelines are known to be more resistant to earthquake damage compared to above-ground structures, but they have suffered severe damage in recent large magnitude earthquakes. Hyogo-Ken Nambu earthquake (1995) led to gas leakage and fires in buried pipelines. Chi-Chi earthquake (1999) caused critical damage to buried natural gas pipeline system (Lee et al., 2009). Trans-Alaska Pipeline System suffered structural damage under 2002 Denali earthquake (Honegger et al., 2004). Damage in pipelines is caused by transient ground deformation and permanent ground deformation due to fault movement, liquefaction, and landslides (ALA, 2001). Typically, the damage caused by transient ground deformation is significantly lower than that caused by permanent ground deformation. However, it may induce damage over a larger area (Toprak et al., 2008). In this study, we focus only on the response of buried pipelines due

to transient ground deformation.

Various studies have been performed to investigate the seismic response characteristics of embedded pipelines. The main differences between the seismic behavior of buried pipelines and above-ground structures have been well documented (Datta, 1999). One of the critical discrepancy is that the motions arriving at the pipeline are incoherent, because of the phase difference at different locations along the pipeline caused by the arrival time delay. Another difference is that the waveforms are altered due to the spatial variability of soil properties surrounding the pipeline and scattering of waves. The effect of spatial variability of soil properties may have an important influence on the seismic response of pipelines, especially at the boundary of two layers with highly contrasting stiffness (Park et al., 2009). However, it is not commonly accounted for and only the effect of phase difference is considered in the design.

The dominant failure mode of pipelines caused by the transient ground motion is reported to be dependent on the type of joint (Psyrras and Sextos, 2018). For welded steel pipelines, five failure modes are defined, which include shell-mode buckling, beam-mode buckling, pure tensile rupture, flexural failure, and

CORRESPONDENCE Duhee Park ✉ dpark@hanyang.ac.kr ☒ Dept. of Civil and Environmental Engineering, Hanyang University, Seoul 04763, Korea

© 2020 Korean Society of Civil Engineers

section ovalization. Because of the ductility of steel pipelines, tensile, flexural, and ovaling failure modes have been demonstrated to be the secondary modes of failure. Both shell and beam buckling failure modes are mobilized by compressive axial force. For segmented pipelines, the critical model of failure is the pull-out of the mechanical joints. Therefore, it can be summarized that the longitudinal strain (acting along the axis of the pipeline) that induces both the compressive and tensile forces is the critical design parameter.

A series of equations and models have been proposed to predict the pipeline response under earthquake loading. The simplest model does not account for the soil-structure interaction. Considering only the time delay, free-field strain and curvature equations were calculated by Newmark (1967). The inertia force and the soil-pipeline interaction were ignored. Hindy and Novak (1979) derived equations for free-field strains and curvature due to incident P and S waves. St John and Zahrah (1987), based on the study of Newmark (1967), summarized free field strains caused by incident P, S, and Rayleigh waves. St John and Zahrah (1987) also proposed closed-form solutions based on beam-on-elastic foundation approach to account for the soil-structure interaction. The solutions do not account for the inertial effects.

Beams have been shown to be inappropriate for modeling the buckling and crack propagation in large diameter pipelines. Shell elements have been used to overcome such limitations (Wong et al., 1986; Luco and De Barros, 1994). The differences between results using shell and beam models used for pipelines were documented by Gantes and Melissianos (2013). Shell models were shown to accurately model the localized buckling and distortion, but required significantly longer computational time. Saberi et al. (2013) reported that the difference in the calculated results using beam and shell models is minor.

Lee et al. (2009) performed 3D dynamic analyses using the frame analysis program ZeusNL (Elnashai et al., 2011) to evaluate the effect of soil type, embedment depth on straight and curved pipelines. Pipeline was modeled with beam elements and elasto-plastic springs were used for the soil. The force-displacement curves of ALA (2001) were used for the springs. The acceleration time histories were applied directly to the springs. The soil type and embedment depth was shown to have important influence on the pipeline. Saberi et al. (2011) performed 3D finite element analyses using Abaqus on pipelines embedded in sands and clays. The shell elements were used for the pipeline and the surrounding soil was modeled with springs. The effect of embedment depth, diameter, soil properties were investigated. Saberi et al. (2013) focused on the deformation of curved pipelines. The curved section was modeled with a shell element, whereas the rest of the pipeline was modeled with beam elements. The influence of the angle of curvature, incident wave angle on axial strain induced in the pipelines was investigated. The results were verified against the regression equations from 2D equivalent linear analyses reported in McLaughlin and O'Rourke (2009).

Although dynamic numerical analyses have been used in research, they are seldom performed in practice. Instead, simplified

empirical procedures are most often used in practice. ALA (2005) proposes to use 1) chart method, 2) equivalent static, 3) finite element approach for seismic design of water pipelines. The chart method provides the recommended joints to be used for various types of water pipelines based on peak ground velocity (PGV). The equivalent static method estimates the peak longitudinal strain from PGV and shear velocity of soil, maximum frictional force acting on pipe barrel. The peak longitudinal strain is applied to the pipeline to evaluate the performance of the pipeline. The procedure does not account for the frequency characteristics of the subjected ground motion and the site conditions. In the finite element approach, the pipeline is modeled by finite elements, whereas the surrounding soil is modeled by 3D springs. The numerical models for the nonlinear springs are also provide in ALA (2001). It was recommended to use this approach for assessment of pipeline damage to permanent ground deformation. A pseudo-static approach accounting for the soil-structure interaction and the seismic site effects is not presented. Empirical pseudo-static procedures have been used for seismic design of tunnels using assumed input ground motion parameters and closed-form solutions to calculate the longitudinal strain in a beam subjected to a harmonic motion. The degree of uncertainty in the estimated tunnel response using the pseudo-static procedure has not yet been documented.

The objective of this study is to develop an enhanced pseudo-static procedure to calculate the longitudinal strain in pipelines caused by transient loading. We perform a parametric study for quantitative comparisons of the pseudo-static and 3D nonlinear time history analysis, which is used as the baseline analysis. The parameters considered are incident plane, transient characteristics of the wave, bi-directional loading, and nonlinear soil response. The causes for the difference between two procedures are identified. Based on extensive comparisons between the pseudo-static and 3D time history analyses, guidelines to predict the longitudinal strain from simplified pseudo-static analysis are presented.

2. Procedures to Calculate Seismic Response of Pipelines Subjected to Incident Shear Wave

Figure 1 is a schematic plot of the pipeline response for free-field condition subjected to a harmonic motion propagating along the horizontal plane (x-y plane) at an angle of incidence θ from the longitudinal axis (x-axis). This harmonic motion produces both axial and transverse deformations. The transverse component causes curvature deformation, inducing a bending strain. The longitudinal strain is caused by both the axial and bending displacements. It should be noted that the longitudinal strain is dependent on the peak amplitude and the wavelength, which in turn is conditioned on the period of vibration of the incident wave and the wave velocity of the ground.

Both pseudo-static and dynamic analyses are used to estimate the longitudinal strain in pipelines. In a pseudo-static approach, the input ground motion parameters are the peak amplitude of

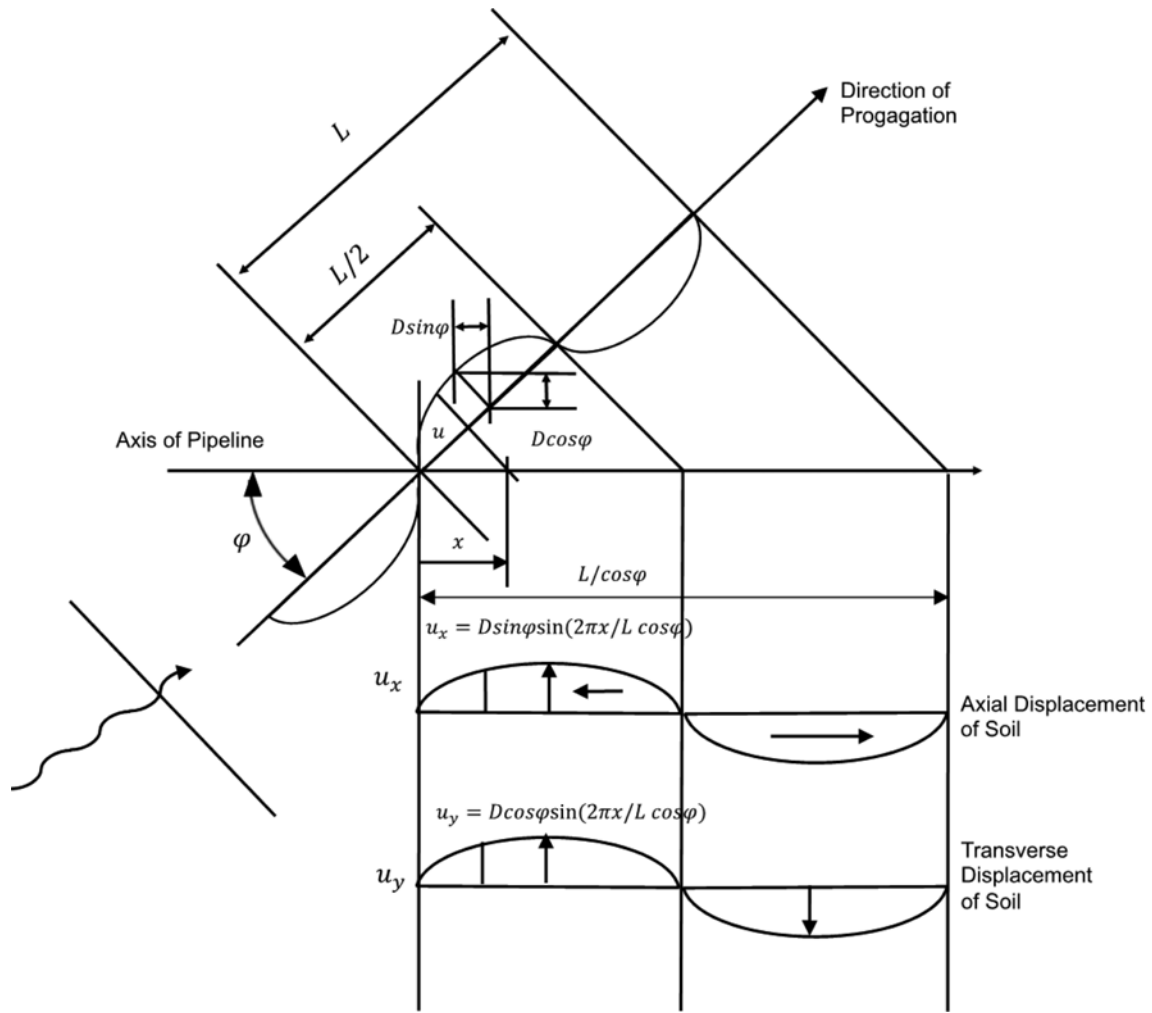


Fig. 1. Free-Field Pipeline Response Subjected to a Harmonic Wave Propagating at an Incident Angle from the Longitudinal Axis (modified after St John and Zahrah, 1987)

ground deformation and the wavelength. Various studies have been performed to predict the peak ground displacement or velocity. Peak ground velocity (PGV)/peak ground acceleration (PGA) and peak ground acceleration (PGD)/PGA ratios were proposed by Power (1966). Other empirical equations include those by Bommer et al. (2000) and Trombetti et al. (2008). A comprehensive literature review on the empirical methods to predict the peak displacement is out of scope of this study. As for the wavelength, Hashash et al. (2001) proposed to determine the wavelength as the product of the predominant period of the ground motion and the shear wave velocity (V_s) of the soil at the depth of the pipeline. The accuracy of this procedure has not yet been evaluated.

The ground motion parameters may be determined empirically or from one-dimensional (1D) site response analysis. The displacement time history at the embedment depth can be extracted and used to determine the ground motion parameters. Closed-form design equations are then used to determine the pipeline response. St John and Zahrah (1987) proposed analytical solutions to calculate strains in the pipelines subjected to harmonic waves for

both the free-field and the soil-pipeline interaction simulated conditions. Axial strain (ϵ^a) and bending strain (ϵ^b) of the pipeline accounting for the soil-pipeline interaction are as follows:

$$\epsilon^a = \frac{\left(\frac{2\pi}{L}\right) A \sin \phi \cos \phi}{2 + \frac{E_i A_c}{K_a} \left(\frac{2\pi}{L}\right)^2 \cos^2 \phi} \cos \left(\frac{2\pi x}{L \cos \phi}\right) \quad (1)$$

$$\epsilon^b = \frac{\left(\frac{2\pi}{L}\right)^2}{1 + \frac{E_i I_c}{K_t} \left(\frac{2\pi}{L}\right)^4 \cos^4 \phi} r A \sin \left(\frac{2\pi x}{L \cos \phi}\right) \quad (2)$$

where L is the wavelength of a harmonic sinusoidal shear wave, A is the free-field amplitude of a harmonic sinusoidal shear wave, E_i is the elastic modulus of an underground structure, A_c is the cross sectional area of an underground structure, I_c is the moment of inertia of an underground structure section, r is the radius of circular underground structure, K_a is the longitudinal spring coefficient of soil medium, K_t is the transverse (horizontal)

spring coefficient of soil medium, x is the longitudinal distance of an underground structure. The primary advantage of a pseudo-static analysis is the ease-of-use. However, it cannot simulate the transient and bi-directional deformation, and nonlinear behavior of soil. The accuracy of the method compared with more rigorous methods needs to be investigated.

In a dynamic analysis, the ground motion is applied to the bottom boundary of the soil model surrounding the pipeline. A three-dimensional (3D) continuum model can realistically capture the complex soil-pipeline interaction, including the nonlinear soil behavior, inelastic pipeline response, and the slip or gapping at the soil-structure interface. However, a majority of commercial continuum analysis programs only allow applying identical motion across the entire bottom domain. Therefore, the spatial variability including the time delay of arriving waves along the length of the pipeline cannot be simulated. In a 3D frame analysis method, the soil is modeled with 3D uncoupled and discrete springs placed at a given spacing. The motion time histories are applied directly to the springs. Therefore, the variation in the ground motion can be easily modeled. Because the spatial variability of the ground motion is the fundamental cause of the induced longitudinal strain, 3D frame analysis method has been widely used to simulate the seismic response of pipelines (Lee et al., 2009).

3. Numerical Simulation

We performed 3D time history analyses of pipelines using the frame analysis software ZeusNL (Elnashai et al., 2011). The numerical model of the pipeline is shown in Fig. 2. The model

consists of the pipeline connected to 3D springs that represent the surrounding soil. The pipeline was modeled as 1 km long beam buried at a depth of 1.5 m using the 3D cubic elastic beam element. The internal pressure within the pipeline was ignored in the analysis. The fixed boundary conditions were applied to both ends of the pipelines. Properties of the steel pipeline, representative of API-5L Grade X80 (API Specification 5L, 2000), are summarized in Table 1. The elasto-plastic models of ALA (2001) were used for the 3D springs attached to the nodes of beam elements. The force – displacement curves of the springs are shown in Fig. 3. The longitudinal and transverse-horizontal springs are represented by symmetric curves, whereas an asymmetric curve is used for the vertical spring. It should be noted that the coefficients are different for the longitudinal, transverse, and lateral springs. The maximum resistance and elastic deformation of springs were calculated separately for clays and sands, following the guidelines presented in ALA (2005) and summarized in Table 2. The readers are referred to API Specification 5L (2000) for the definition of the factors listed in the equations. The friction angle was determined by firstly using the empirical equation of Kwak et al. (2015) to determine the equivalent standard penetration test blow count and secondly using the equation of Wolff (1989) to estimate the friction angle. The undrained shear strength was determined from the empirical correlation between V_s and undrained shear strength (L'heureux and Long, 2017). K_o was set to 0.5.

The displacement time histories were applied to the transverse and vertical springs. The time history analysis is essentially a static analysis, but the temporal variation of a transient displacement time series can be modeled. Contrary to a dynamic analysis, it

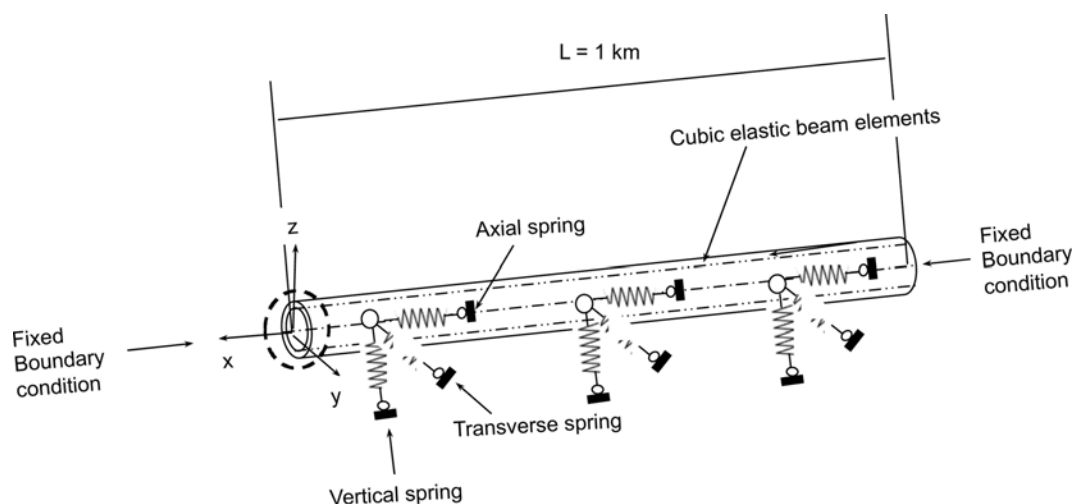


Fig. 2. Numerical Model of the Pipeline and the Surrounding Soil

Table 1. Material Properties

Pipe type	Diameter (m)	Thickness (mm)	Buried depth (m)	Elastic modulus (GPa)	Yield strength (MPa)	Poisson ratio (ν)
Steel API 5L X80	1.219	20	1.5	200	625	0.3

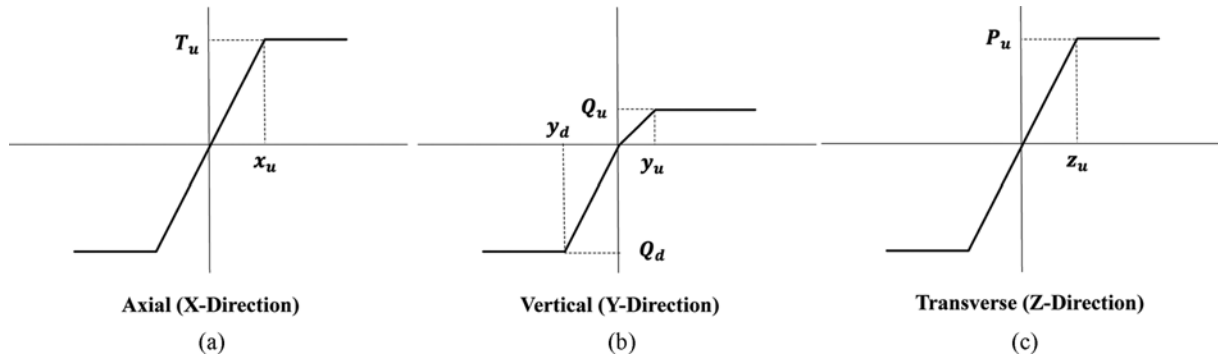


Fig. 3. Force-Displacement Relationships of Soil Springs (modified after ALA, 2001): (a) Axial Direction, (b) Vertical Direction, (c) Transverse Direction

Table 2. The Force-Displacement Relationship of Soil Spring (ALA, 2001)

Direction	Clay		Sand	
	Max. resistance (N/mm)	Max. elastic deformation (mm)	Max. resistance (kN/m)	Max. elastic deformation (mm)
Axial	$t_u = \pi D \alpha s_u$	$x_u = 9$	$t_u = \frac{\pi}{2} D \gamma H (1 + K_0) \tan \phi$	$x_u = 4$
Transverse (Horizontal)	$p_u = s_u N_{ch} D$	$y_u = 0.04 \left(H + \frac{D}{2} \right)$	$p_u = \gamma H N_q D + \frac{1}{2} \gamma D^2 N_\gamma$	$y_u = 0.04 \left(H + \frac{D}{2} \right)$
Transverse (Vertical) Upward	$q_u = s_u N_{cV} D$	$z_u = (0.0125) H$	$q_u = \gamma H N_q D$	$z_u = (0.15) H$
Transverse (Vertical) Downward	$q_d = s_u N_c D$	$z_u = (0.125) D$	$q_u = \gamma H N_q D + \frac{1}{2} \gamma D^2 N_\gamma$	$z_u = (0.125) D$

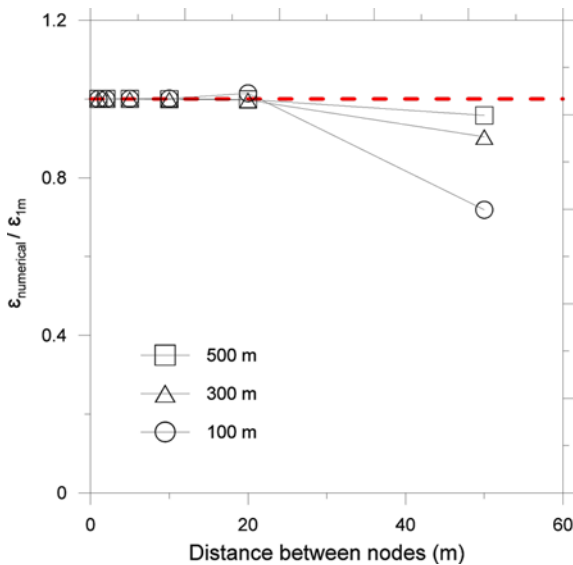


Fig. 4. Sensitivity of Numerically Calculated Longitudinal Strain ($\epsilon_{\text{numerical}}$) on Beam Element Length (spring spacing) ($\epsilon_{\text{numerical}}$ is normalized by the maximum strain calculated using element length = 1 m.)

does not impose inertial force on the pipelines. Dynamic analyses were not performed, because it was reported that the dynamic amplification of underground structures is not significant and a

pseudo-static analysis provides sufficiently accurate estimate for engineering practice (Hashash et al., 2001). To consider the wave passage effect, we adopted the methodology outlined in Eurocode8 (EN 1998-1, 2004). At point x_i along the longitudinal axis of the pipeline, the seismic waves will propagate with a time lag t_i .

$$t_i = x_i / C_\alpha \tag{3}$$

where C_α is the apparent wave velocity defined as follows:

$$C_\alpha = V_s / \sin \beta_s \tag{4}$$

where β_s is incidence angle, V_s is shear wave velocity of the soil at the depth of the pipeline. For a conservative estimate, $\beta_s = 45^\circ$ was used in all analyses.

We evaluated the boundary effect, the output of which is depicted in Fig. 5. The maximum strains were calculated at each beam element along the pipeline, again using three harmonic motions with different wavelengths. The strain is normalized by the longitudinal strain at the mid-point of the 1 km long beam. At a distance of 70 m from the fixed ends, the calculated strain is shown to converge. It is demonstrated that the strain calculated at a distance less than 70 m from the fixed end should not be used in design, unless such a case is specifically simulated. We extracted the longitudinal strain at the middle of the pipeline.

For verification of the numerical model, the outputs are compared with those from the closed-form solution of St John

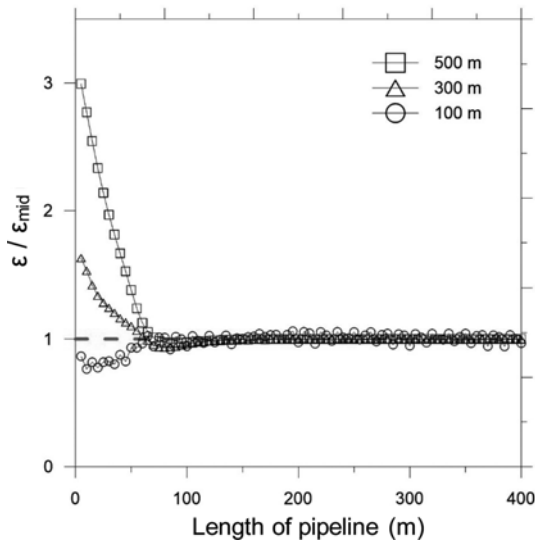


Fig. 5. Maximum Longitudinal Strain Calculated along the Pipeline (The longitudinal strain is normalized to the strain at the middle of the pipeline.)

and Zahrah (1987). For the numerical model, linear elastic springs were used for comparison purposes. A series of harmonic motions with amplitudes ranging from 100 to 1,000 mm and wavelengths from 50 to 900 m were applied at an incident angle of 45° . V_s of the soil was set to 100 and 300 m/s. Fig. 5 shows that the numerically calculated longitudinal strains at the center of the 1 km long pipeline and those from the analytical equation are almost identical. The comparisons demonstrate that the 3D numerical model provides accurate estimate of the pipeline response.

4. Parametric Study

A parametric study was carried out to investigate the degree of influence of four parameters on the calculated pipeline response for a given set of input ground motions. The parameters considered are 1) incident plane, 2) transient characteristics of the wave, 3) bi-directional loading, and 4) pipeline-soil interface. The input displacement time histories were calculated from a suite of 1D

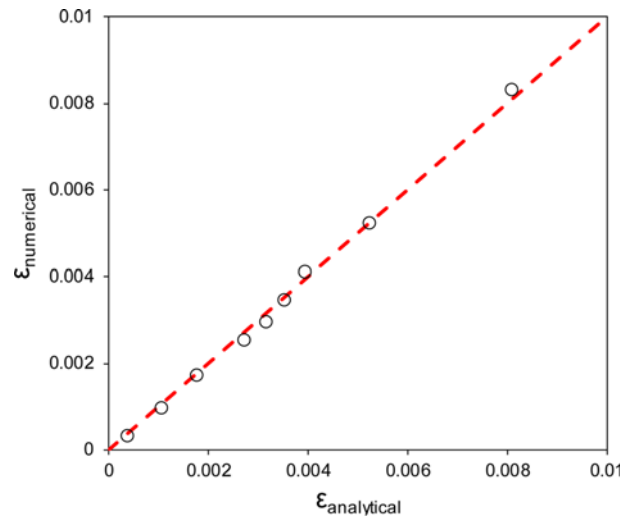


Fig. 6. Comparison of the Longitudinal Strains Calculated from the Numerical Model Using Linear Elastic Model for Soil Springs and the Analytical Solution

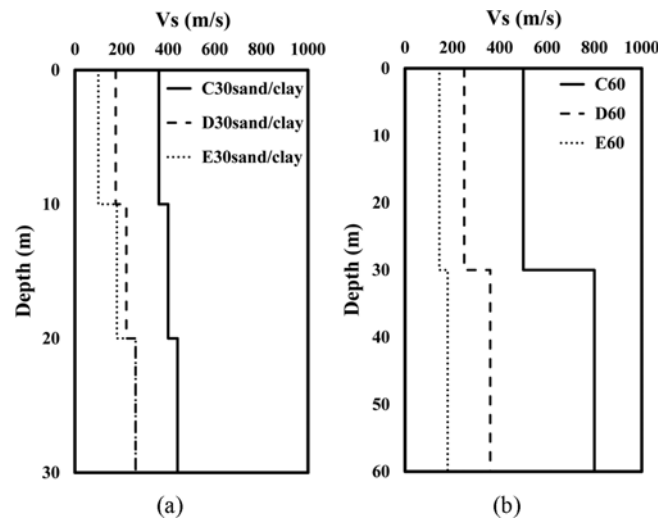


Fig. 7. Site Profiles Used in the Analyses (The profiles are from Argyroudis and Ptilakis (2012)): (a) 30 m in Thickness, (b) 60 m in Thickness

site response analyses. A total of nine idealized soil profiles taken from the study of Argyroudis and Ptilakis (2012), as

Table 3. Recorded Motions Used in the Analyses

Earthquake	Station	Magnitude	Fault mechanism	V_{s30} (m/s)
Chi-Chi (1999)	HWA002	7.6	Reverse oblique	789
Coyote Lake (1979)	Gilroy Array	5.7	Strike-slip	1,428
Hollister (1974)	Gilroy Array	5.1	Strike-slip	792
Kocaeli (1999)	Gebze	7.5	Strike-slip	811
Kocaeli (1999)	Izmit	7.5	Strike-slip	811
Loma Prieta (1989)	Mont school	6.9	Reverse oblique	895
Morgan Hill (1984)	Gilroy Array	6.2	Strike-slip	1,428
Northridge (1994)	VRP	6.7	Reverse	996
San Francisco (1957)	Golden Gate park	5.3	Reverse	874
Umbria (1984)	Gubbio	5.6	Normal	922

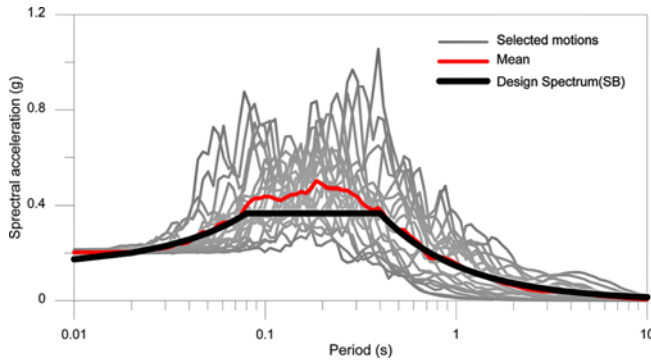


Fig. 8. 5% Damped Acceleration Response Spectra of Input Ground Motions Scaled to PGA = 0.2 g

displayed in Fig. 7, were used. The profiles range from 30 m to 60 m in thickness, 0.3 to 0.9 s in T_{ss} , and 153 to 397 in V_{s30} . 30 m thick profiles consist of either uniform sand or clay layers. 60 m profile is composed of 5 m thick sand layer underlain by clay layers. Ten sets of input ground motions were used. Each set consists of two horizontal components. P wave was not used because it was reported to have a secondary influence on the response of pipelines (Anastasopoulos et al., 2007). The details of the recorded motions are summarized in Table 3. The motions were scaled to four levels of peak ground accelerations (PGAs), which are 0.2, 0.4, 0.6, and 0.8 g. The 5% damped acceleration response spectra scaled to 0.2 g are shown in Fig. 8. The number of scaled motions used was 80. A total of 720 site response analyses was performed. Equivalent linear site response analyses were performed using Deepsoil (Hashash et al., 2017). Nonlinear curves of Darendeli (2001) were used for both sand and clay layers. For clay layers, PI = 30 and OCR = 1 were assumed. V_s of the bedrock was set to 1,500 m/s. The acceleration, velocity, and displacement time histories were calculated at a depth of 1.5 m. The displacement time histories calculated at a depth of 1.5 m were extracted. The calculated longitudinal strain is normalized by the critical strain, which is defined as follows ALA (2005).

$$\epsilon_{cr} = 0.175 \frac{t}{R} \tag{5}$$

where t is the thickness and R is the radius of the pipeline.

4.1 Effect of Incident Plane

Selected sets of analyses were performed to evaluate the effect of the incident plane on the pipeline response. Horizontal shear (SH) and vertical shear (SV) motions were applied on horizontal and vertical planes, respectively, to induce both curvature and axial strains. Harmonic motion with a period of vibration from 0.25 to 3.0 s and an amplitude of 100 mm was subjected at an incident angle of 45° from the longitudinal axis of the pipeline. V_s and ϕ of the soil were set to 100 m/s and 28°, respectively. Fig. 9 compares the normalized longitudinal strains calculated from two sets of simulations. The maximum residual between the calculated strains is 4%. This is caused by the difference in the coefficients of vertical and transverse springs. Although the

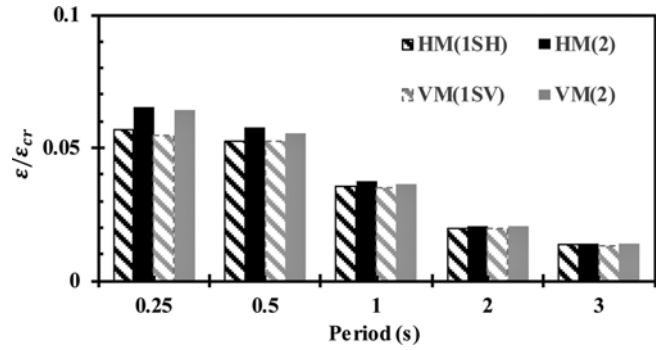


Fig. 9. Calculated Normalized Longitudinal Strain in the Pipeline Subjected to Various Combinations of Harmonic Motions: HW(1SH) = SH Wave on horizontal Plane, VM(1SV) = SV Wave on Vertical Plane, HM(2) = SH and SV Waves on Horizontal Plane, VM(2) = SH and SV Waves on Vertical Plane

discrepancy is not pronounced, the motions applied on the horizontal plane result in slightly higher responses. All motions were applied on the horizontal plane in the following sections, except when applying the bi-directional loading.

4.2 Effect of Bi-Directional Loading

We applied bi-directional motions and compared the responses with those subjected to uni-directional loadings. For bi-directional loadings, SH and SV waves were simultaneously imposed to transverse and vertical springs, respectively. The results using harmonic motions are displayed in Fig. 9. Compared with the outputs for uni-directional loadings, application of the bi-directional loadings produce up to a 12% increase in the combined strain. In addition to harmonic motions, two horizontal components of the transient motions were also applied in the form of bi-direction loading. Fig. 10 compares the normalized longitudinal

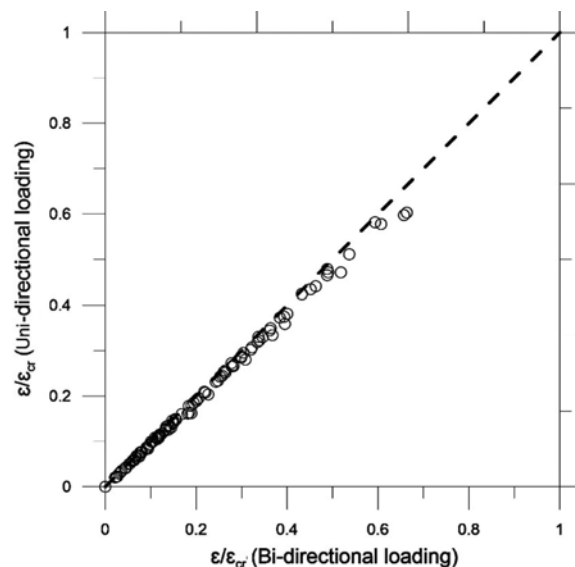


Fig. 10. Comparison of Normalized Longitudinal Strains in Pipelines Subjected to Uni-Directional and Bi-Directional Loadings

strains subjected to uni- and bi-directional loadings. The median difference between two sets of analyses is 4.3% and the maximum difference is 11.6%. The median difference produced by the transient motions is smaller than the result using harmonic motions, because of the incoherency between two components of the recorded ground motions.

4.3 Effect of Elasto-Plastic Soil Model

In this section, we evaluate the influence of the elasto-plastic soil model on the calculated response. We compare the results of numerical simulation using 3D elasto-plastic springs and the closed-form solution of St John and Zahrah (1987). In the analytical solution, the soil is modeled as a linear elastic material.

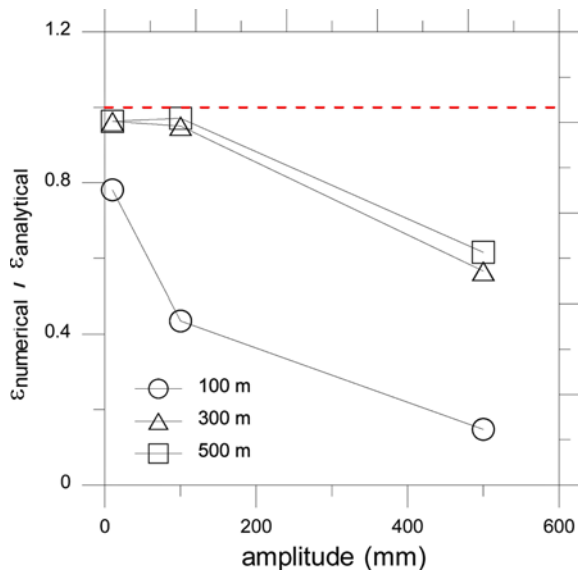


Fig. 11. Comparison of Ratio of Strains Calculated from Numerical Simulations with the Closed-Form Solution of St John and Zahrah (1987)

As noted in the previous section, the coefficients for longitudinal, lateral, and vertical springs all differ in the numerical model. The numerical model simulates more realistically the pipeline-soil interaction compared with the simplified elastic model. The closed-form solution, however, is easier to use in practice.

A broad range of amplitudes and wavelengths were applied to compare the results of two types of analyses. The amplitudes used were 10, 100, and 500 mm. The wavelength was varied from 200 m to 1,500 m. V_s was assumed as 150, 300, and 500 m/s. The Poisson's ratio was set to 0.3. Fig. 11 compares the axial strains calculated by the analytical equation and the numerical simulation. Comparisons show that two types of analyses result in similar responses for low amplitudes and long wavelengths. The differences are negligible for wavelengths 300 and 500 m and peak amplitude up to 100 mm. The numerically calculated strain quickly decreases at higher amplitudes. For the shortest wavelength, the difference occurs even at a peak amplitude of 10 mm. The comparisons highlight that the elastic solution overestimates the longitudinal strain for short wavelength and high amplitude ground motions.

4.4 Transient Motion versus Equivalent Harmonic Motion

In this section, we evaluate whether a transient motion with non-stationary characteristics can be approximated with an equivalent harmonic motion in calculating the pipeline response. If this is possible, a pseudo-static analysis may be used instead of a time history analysis to evaluate the seismic performance of pipelines. A total of twenty displacement time histories, calculated from site response analyses using two soil profiles (D30 and E30) and ten input ground motions, were used. The equivalent harmonic motion was generated using the peak pulse of the transient displacement time history.

Figure 12(a) compares the longitudinal strains calculated from two sets of analyses. The ratio of the longitudinal strain subjected to an equivalent harmonic motion ($\epsilon_{\text{harmonic}}$) to the strain due to a

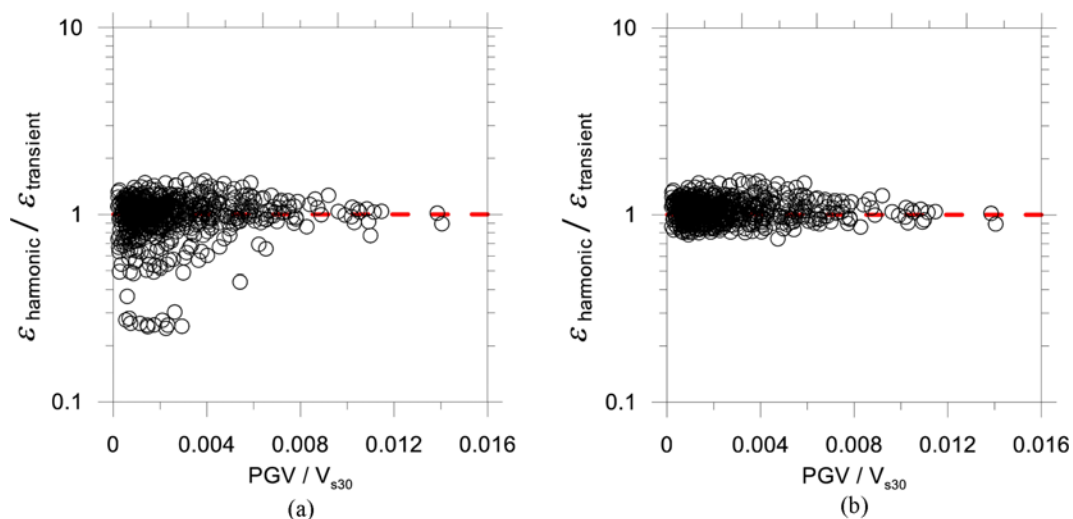


Fig. 12. Ratio of Longitudinal Strains Subjected to Equivalent Harmonic and Transient Motions: (a) Equivalent Harmonic Motion Generated Using Peak Pulse, (b) Equivalent Harmonic Motion Generated Using a Pulse That Induces Peak Strain

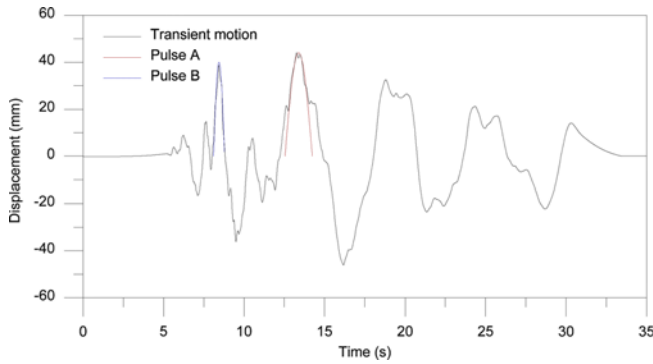


Fig. 13. Displacement Time History and Peak Pulses

transient motion ($\epsilon_{\text{transient}}$) is plotted against PGV / V_{s30} . The ratios are smaller than unity for a large portion of the analyses, demonstrating that an equivalent harmonic motion generated using the peak pulse is likely to result in a lower response. The cause for this discrepancy can be explained by the displacement time history shown in Fig. 13. The peak pulse is designated with the letter A in the figure. Pulse B, also shown in Fig. 13, is lower than Pulse A in amplitude, but has a much shorter duration. Because of this shorter duration, it induces a higher longitudinal strain. Therefore, when generating an equivalent harmonic motion, the pulse that induces the largest longitudinal strain should be selected. Fig. 12(b) present results that use this procedure to generate the equivalent harmonic motions. The ratio of calculated strains using transient motions and equivalent harmonic motions range from 0.75 to 1.53. In this study, the procedure using the peak amplitude of the displacement time history to determine both the displacement amplitude and the wavelength is termed as the *peak amplitude method*. The procedure using the pulse that induces the largest longitudinal strain considering both the amplitude and the duration is denoted as the *peak strain method*. Both methods are used to calculate the longitudinal strains for a suite of analyses, presented in the following section.

5. Prediction of Longitudinal Strain

As discussed previously, it is not always possible to run a 3D time history analysis to predict the longitudinal strain. In this section, we use various alternative empirical procedures to estimate the longitudinal strain. The accuracy of each method is evaluated through comparison with the numerical simulation outputs.

We used 720 displacement time histories calculated from 1D site response analyses, as documented in the previous section.

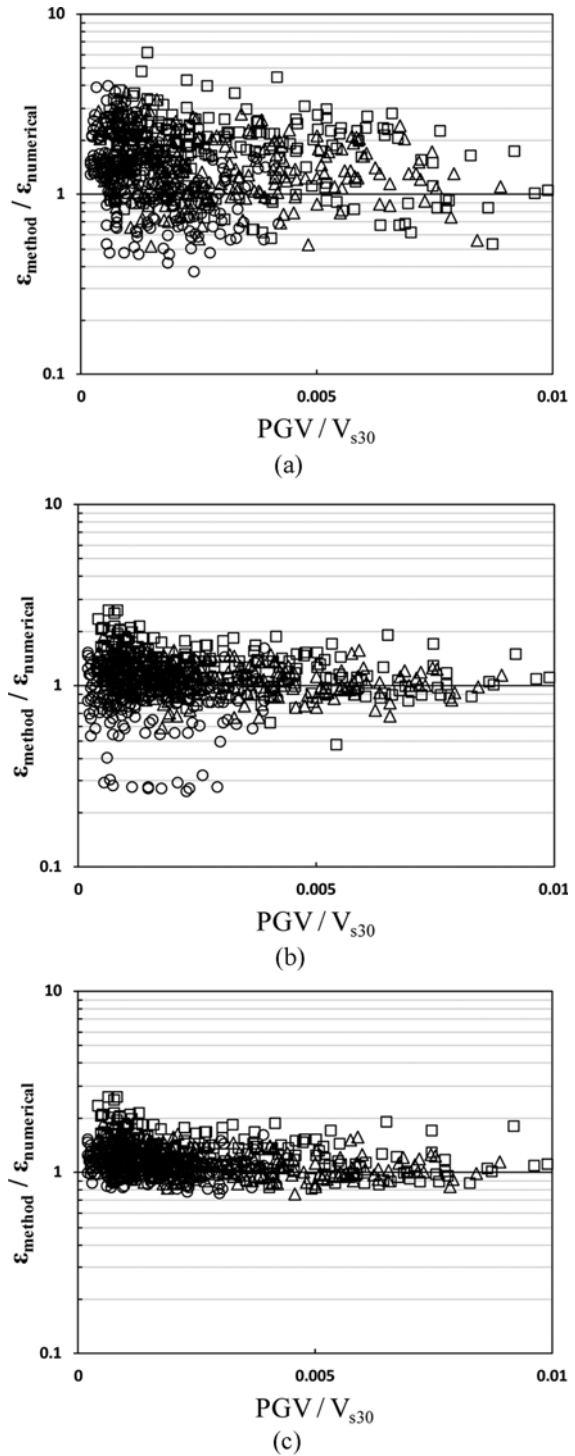


Fig. 14. Comparison between Calculated Strains from Time History Analyses Normalized by Those from Empirical Methods: (a) Method A, (b) Method B, (c) Method C

Table 4. Empirical Procedures to Estimate Longitudinal Strain Induced in Pipelines

	Amplitude	Wavelength	Longitudinal strain calculation
Method A	Cosine method	$V_s \times T_s$	St John and Zahrah (1987)
Method B	Site response analysis (Peak amplitude method)		St John and Zahrah (1987)
Method C	Site response analysis (Peak strain method)		St John and Zahrah (1987)

The results of all numerically calculated strains are plotted against PGV/V_{s30} in Fig 11. We further compare the numerical result with three additional empirical procedures, which are termed Method A, B, and C, as summarized in Table 4. Methods A uses the cosine method to determine the peak displacement, which uses the following empirical equation (Railway Technical Research Institute, 1999):

$$U_h(x) = \frac{2}{\pi^2} \cdot S_v \cdot T_s \cdot \cos\left(\frac{\pi}{2H_s} \cdot x\right) \quad (6)$$

where $U_h(z)$ is the horizontal displacement at depth z , S_v is the rock outcrop spectral velocity at site period (T_s), H_s is the thickness of soil profile. In Method A, the wavelength is calculated as the product of T_s and V_s . Both Method B and C use the site response analysis results to estimate the displacement amplitude and wavelength. Method B uses the peak amplitude method to estimate both the displacement amplitude and wavelength. Method C utilizes the peak strain procedure. All methods use the closed-form equation of St John and Zahrah (1987) to calculate the longitudinal strain from calculated amplitude and wavelength. The soil-pipeline interface is not simulated and therefore will overestimate the longitudinal strain in all approximations. Fig. 14 plots the ratio of the empirically determined strain to the numerically calculated strain against PGV/V_{s30} . Method A is shown to produce a wide scatter of the ratio. Cosine method and T_s of the site profile is shown to provide inaccurate estimate of the longitudinal strain. The scatter of the data is significantly reduced when Method B is used, because the prediction of the amplitude and wavelength is greatly improved. However, Method C shows the lowest scatter in the prediction and mostly provides conservative estimates. Comparison of Method B and C demonstrates that in addition to reliable estimate of the peak amplitude, determination of the wavelength is important.

As reported in previous section, the closed-form solution produces more conservative estimate of the longitudinal strain compared with the numerical solution, because of the linear response assumption for the surrounding soil. Therefore, even though the ground motion parameters are accurately estimated, it still produces conservative estimate of the longitudinal strain. However, because it mostly provides a conservative estimate, the procedure is suitable to be used in design.

6. Conclusions

We performed 1D site response analyses and 3D time history analyses to calculate the longitudinal strain of buried pipelines subjected to seismic motions. We also performed parallel simplified pseudo-static analyses to predict the response of the pipelines. The conclusions of this study are summarized in the following.

1. The closed-form solution is demonstrated to provide conservative estimate of the longitudinal strain compared to a 3D time history analysis when identical harmonic motion is applied. This is because the soil is modeled as a linear elastic material, whereas the time history analysis

uses 3D elasto-plastic springs.

2. A transient motion can be approximated as an equivalent harmonic motion. However, caution is warranted in the approximation procedure. Use of the peak amplitude pulse from the transient motion to develop the equivalent harmonic motion may produce an underestimation of the longitudinal strain. It is recommended to extract a pulse that induces the largest strain considering both the amplitude and the duration, the procedure of which is termed as the *peak strain method*.
3. The incident plane and bi-directional loading are shown to have marginal influences on the calculated response. It is therefore concluded that the current practice of applying uni-directional loading on horizontal plane is acceptable.
4. The accuracies of three design procedures to predict the longitudinal strain in pipelines are evaluated. All procedures use the closed form solution to calculate the strain for a given peak amplitude and period of vibration. Method A, which uses the site period to determine the wavelength and the amplitude is estimated from the empirical cosine method, provides highly conservative estimate of the longitudinal strain. Method B, which uses the site response analysis output to determine the peak amplitude and associated wavelength, highly underestimates the induced strain. The longitudinal strain is most favorably predicted by Method C, which uses the *peak strain method* to extract the input ground motion parameters for the closed-form equation from the site response analysis results.
5. Use of the simplified pseudo-static method involves inherent uncertainties. However, the error using Method C that utilizes 1D site response analysis output and the peak strain method is shown to be acceptable for engineering purposes.

Acknowledgements

This research was supported by Basic Science Research Program through the National Research Foundation of Korea (NRF) funded by the Ministry of Science, ICT and Future Planning (NRF-201900000000551) and by a grant (18SCIP-B146946-01) from Construction technology research program funded by Ministry of Land, Infrastructure and Transport of Korean government.

ORCID

Duhee Park  <https://orcid.org/0000-0002-0180-2668>

References

- ALA (2001) Guideline for the design of buried steel pipe. American Society of Civil Engineers and Federal Emergency Management Agency, American Lifeline Alliance, Washington, DC, USA
- ALA (2005) Seismic guidelines for water pipelines. National Institute of Building Sciences and Federal Emergency Management Agency,

- American Lifelines Alliance, Washington, DC, USA
- Anastasopoulos I, Gerolymos N, Drosos V, Kourkoulis R, Georarakos T, Gazetas G (2007) Nonlinear response of deep immersed tunnel to strong seismic shaking. *Journal of Geotechnical and Geoenvironmental Engineering* 133(9):1067-1090, DOI: 10.1061/(ASCE)1090-0241(2007)133:9(1067)
- API Specification 5L (2000) Specification for line pipe, 42nd edition. American Petroleum Institute, Washington, DC, USA
- Argyroudis SA, Ptilakis KD (2012) Seismic fragility curves of shallow tunnels in alluvial deposits. *Soil Dynamics and Earthquake Engineering* 35(4):1-12, DOI: 10.1016/j.soildyn.2011.11.004
- Bommer JJ, Elnashai AS, Weir AG (2000) Compatible acceleration and displacement spectra for seismic design codes. Proceedings of 12th world conference on earthquake engineering, January 30-February 4, Auckland, New Zealand
- Darendeli MB (2001) Development of a new family of normalized modulus reduction and material damping curves. PhD Thesis, University of Texas, Austin, TX, USA
- Datta TK (1999) Seismic response of buried pipelines: A state-of-the-art review. *Nuclear Engineering and Design* 192(2-3):271-284, DOI: 10.1016/S0029-5493(99)00113-2
- Elnashai AS, Papanikolaou VK, Lee DH (2011) Zeus NL - A system for inelastic analysis of structures, user's manual. Mid-America Earthquake Center, Department of Civil and Environmental Engineering, University of Illinois at Urbana-Champaign, Urbana, IL, USA
- EN 1998-1 (2004) Eurocode 8: Design of structures for earthquake resistance – Part 1: General rules, seismic actions and rules for buildings. EN 1998-1, Comité Européen de Normalisation, Brussels, Belgium
- Gantes CJ, Melissianos V (2013) Numerical analysis of buried steel pipelines. Proceedings of 2nd international Balkans conference on challenges of civil engineering, May 23-25, Tirana, Albania
- Hashash YMA, Hook JJ, Schmidt B, John I, Yao C (2001) Seismic design and analysis of underground structures. *Tunnelling and Underground Space Technology* 16(4): 247-293, DOI: 10.1016/S0886-7798(01)00051-7
- Hashash YMA, Musgrove M, Harmon J, Okan I, Groholski D, Phillips C, Park DH (2017) DEEPSOIL 7.0, user manual. University of Illinois at Urbana-Champaign, Champaign, IL, USA
- Hindy A, Novak M (1979) Earthquake response of underground pipelines. *Earthquake Engineering & Structural Dynamics* 7(5):451-476, DOI: 10.1002/eqe.4290070506
- Honegger DG, Nyman DJ, Johnson ER, Cluff LS, Sorensen SP (2004) Trans-Alaska pipeline system performance in the 2002 Denali Fault, Alaska, earthquake. *Earthquake Spectra* 20(3):707-738, DOI: 10.1193/1.1779239
- Kwak DY, Brandenberg SJ, Mikami A, Stewart JP (2015) Prediction equations for estimating shear-wave velocity from combined geotechnical and geomorphic indexes based on Japanese data set. *Bulletin of the Seismological Society of America* 105(4):1919-1930, DOI: 10.1785/0120140326
- Lee DH, Kim BH, Lee H, Kong JS (2009) Seismic behavior of a buried gas pipeline under earthquake excitations. *Engineering Structures* 31(5):1011-1023, DOI: 10.1016/j.engstruct.2008.12.012
- L'heureux JS, Long M (2017) Relationship between shear-wave velocity and geotechnical parameters for Norwegian clays. *Journal of Geotechnical and Geoenvironmental Engineering* 143(6):04017013, DOI: 10.1061/(ASCE)GT.1943-5606.0001645
- Luco JE, De Barros FCP (1994) Seismic response of a cylindrical shell embedded in a layered viscoelastic half-space. I: Formulation. *Earthquake Engineering & Structural Dynamics* 23(5):553-567, DOI: 10.1002/eqe.4290230507
- McLaughlin P, O'Rourke M (2009) Strain in pipe elbows due to wave propagation hazards. Technical council on lifeline earthquake engineering conference (TCLEE) 2009, June 28-July 1, Oakland, CA, USA, 1-11, DOI: 10.1061/41050(357)37
- Newmark NM (1967) Problem in wave propagation in soil and rock. Proceedings of international symposium on wave propagation and dynamic properties of earth materials, August 23-25, Albuquerque, NM, USA
- Park D, Sagong M, Kwak DY, Jeong CG (2009) Simulation of tunnel response under spatially varying ground motion. *Soil Dynamics and Earthquake Engineering* 29(11-12):1417-1424, DOI: 10.1016/j.soildyn.2009.05.005
- Power DV (1966) A survey of complaints of seismic-related damage to surface structures following the Salmon underground nuclear detonation. *Bulletin of the Seismological Society of America* 56(6):1413-1428
- Psyras N, Gerasimidis S, Kwon OS, Sextos AG (2018) Can a buried natural gas pipeline buckle locally during earthquake ground shaking? *Soil Dynamics and Earthquake Engineering* 116:511-529, DOI: 10.1016/j.soildyn.2018.10.027
- Railway Technical Research Institute (1999) Seismic design for railroad structures and commentary. Railway Technical Research Institute, Maruzen, Tokyo, Japan
- Saberi M, Behnamfar F, Vafaeian M (2013) A semi-analytical model for estimating seismic behavior of buried steel pipes at bend point under propagating waves. *Bulletin of Earthquake Engineering* 11(5):1373-1402, DOI: 10.1007/s10518-013-9430-y
- Saberi M, Halabian AM, Vafaeian M (2011) Numerical analysis of buried steel pipelines under earthquake excitations. Proceedings of conference on Pan-Am CGS geotechnical conference, October 2-6, Toronto, Canada
- St-John CM, Zahrah TF (1987) Aseismic design of underground structures. *Tunnelling and Underground Space Technology* 2(2):165-197, DOI: 10.1016/0886-7798(87)90011-3
- Toprak S, Koc A, Cetin O, Nacaroglu E (2008) Assessment of buried pipeline response to earthquake loading by using GIS. Proceedings of 14th world conference of earthquake engineering, October 12-17, Beijing, China
- Trombetti T, Silvestri S, Gasparini G, Pintucchi B, De Stefano M (2008) Numerical verification of the effectiveness of the "Alpha" method for the estimation of the maximum rotational elastic response of eccentric systems. *Journal of Earthquake Engineering* 12(2):249-280, DOI: 10.1080/13632460701385374
- Wolff TF (1989) Pile capacity prediction using parameter functions. Conference of predicted and observed axial behavior of piles: Results of a pile prediction symposium, June 25, Evanston, IL, USA
- Wong KC, Datta SK, Shah AH (1986) Three-dimensional motion of buried pipeline. I: Analysis. *Journal of Engineering Mechanics* 112(12):1319-1337, DOI: 10.1061/(ASCE)0733-9399(1986)112:12(1319)